Article

Fuzzy Rule Based Adaptive Block Compressive Sensing for WSN Application

Dibyalekha Nayak [1], Kananbala Ray [1], Tejaswini Kar [1] and Sachi Nandan Mohanty [2,*]

1   School of Electronics Engineering, KIIT Deemed to be University, Bhubaneswar 751024, Odisha, India
2   School of Computer Science & Engineering, VIT-AP University, Amaravati 522237, Andhra Pradesh, India
*   Correspondence: sachinandan.m@vitap.ac.in

Abstract: Transmission of high volume of data in a restricted wireless sensor network (WSN) has come up as a challenge due to high-energy consumption and larger bandwidth requirement. To address the issues of high-energy consumption and efficient data transmission adaptive block compressive sensing (ABCS) is one of the optimum solution. ABCS framework is well capable to adapt the sampling rate depending on the block's features information that offers higher sampling rate for less compressible blocks and lower sampling rate for more compressible blocks In this paper, we have proposed a novel fuzzy rule based adaptive compressive sensing approach by leveraging the saliency and the edge features of the image making the sampling rate selection completely automatic. Adaptivity of the block sampling ratio has been decided based on the fuzzy logic system (FLS) by considering two important features i.e., edge and saliency information. The proposed framework is experimented on standard dataset, Kodak data set, CCTV images and the Set5 data set images. It achieved an average PSNR of 34.26 and 33.2 and an average SSIM of 0.87 and 0.865 for standard images and CCTV images respectively. Again for high resolution Kodak data set and Set 5 dataset images, it achieved an average PSNR of 32.95 and 31.72 and SSIM of 0.832 and 0.8 respectively. The experiments and the result analysis show that proposed method is efficacious than the state of the art methods in both subjective and objective evaluation metrics.

Keywords: block compressive sensing (BCS); fuzzy decision; saliency detection; edge detection

MSC: 94A08; 03B52

1. Introduction

The wireless sensor network have been successfully applied to different fields, such as disaster management, medical investigation, military battlefield, surveillance and home automation [1–3]. However, the WSN lags in handling huge amount of image data due to the bandwidth and energy limitation as higher the complexity of the process greater the energy requirement [1,3]. To avoid the large data transmission efficient compression is very much essential which will be suitable for WSN application. Compressive sensing (CS) based compression is most widely used compression technique in the WSN [4–7]. In contrast to the scalar data such as temperature, soil moisture etc. image data put much more burden in the WSN transmission and also poses the challenges due to their restricted resources. Therefore, the compression of the raw image is highly required to save the energy and space. Different image compression algorithms, which are based on the transform based approach and follow the Nyquist sampling theorems (i.e., JPEG [8], JPEG2000 [9]), are not applicable for the restricted WSN application. JPEG [8] and JPEG2000 [9] are not preferable in the restricted WSN because of its coding complexity, power consumption and channel errors. The Compressive sensing (CS) [10] is a decade old technique, which doesn't follow the Nyquist sampling theorem and is suitable for both data acquisition and compression. The CS provides sampling and compression as a related process rather than

the two separate process. The study of CS revealed that the signal can still be recovered even from a lower number of samples. At the time of transmission data loss occur in WSN due to the multi path processing. However with CS the complete data can be recovered from the insufficient data with minimal loss [4–6]. This sampled data recovery system of CS and advantages of adaptive BCS have motivated us to design an automatic and adaptive block image compression algorithm based on CS for WSNs.

Since CS based approach deals with vectored representation of the image, it becomes difficult to handle the complete image at a time. The solution is to use block-based approach of compressive sensing through BCS [11] instead of processing the complete image in one go. Due to block-based processing, the size of the sampling matrix is also small that lead to lower computational complexity. Here the sampling matrix size is fixed for all the blocks. Since, the image blocks are varying according to their feature content, applying a fixed sampling ratio for all the blocks is not an optimum choice. Considering this, Adaptive Block Compressive Sensing (ABCS) [12] technique is developed where the blocks with higher feature content block should be compressed at lower rate than the blocks with lower feature content to maintain the clarity of the reconstructed image and to restore the data loss. In the ABCS method, the selection of the blocks was done by using a threshold value depending on the feature content of the block.

2. Related Work

This section describes the literature review related to different CS based approaches for image compression. Monika, et al. [12] proposed a review on ABCS method which gives the detailed description regarding the challenges and different adaptivity consideration for block selection. Zha, et al. [13] proposed Discrete Cosine Transform (DCT) based sparsity computation followed by sparsity dependent ABCS method. Here the sampling rate output will be any of the four predetermined levels. Therefore, it is not completely automatic image adaptive sampling ratio detection method. Monika, et al. [14] proposed coefficient permuted ABCS method suitable for under water WSN using fewer samples. Xu, et al. [15] proposed an adaptive perceptual BCS scheme which combines sparsity and perceptual sensibility to decide the sampling rate allocation of the blocks. Heng, et al. [16] proposed a fuzzy logic based ABCS method by considering the standard deviation and sparsity of the image block. The authors have also developed a fuzzy based recovery algorithm that maintains the quality of the reconstruction. This method is efficient in terms of quality of the reconstruction. However the authors are silent about the complexity analysis. Sum, et al. [17] proposed texture feature based approach for adaptivity of the blocks which may not be suitable for all varieties of images. Many saliency based the ABCS approaches [18–20] can be found in the literature, where the authors used saliency information for deciding adaptivity of the blocks. Different saliency detection approaches can be found in the literature [21–23] which are used for wild life monitoring.

In the literature authors have applied different features such as entropy [24], wavelet co-efficient [25], standard deviation [26] to find the adaptive sampling ratio of the blocks suitable for gray scale images. These methods were successful in maintaining the quality of the reconstructed image. Zhao, et al. [27] proposed gradient based ABCS method However it suffers from blocking artifacts in the reconstructed image. Zhao, et al. [28] proposed multi shaped block strategies based adaptive block sampling ratio for real time application on IoT. Due to the use of different block sizes, it increases the burden on the processor. Canh, et al. [29] proposed an edge preserving CS recovery technique by considering the nonlocal and the histogram information of the image in the form of gradient. The method doesn't have much significant improvement over existing methods [12]. Li, et al. [30] proposed an adaptive block sampling rate detection method by considering the error between the blocks. However, reconstructed image has poor quality. Monika, et al. [31] proposed an energy adaptive block selection based ABCS method. As this method has less energy consumption, hence suitably applied for underwater based IoT images. Gambhir, et al. [32] proposed the edge and fuzzy transform based image compression using the

standard deviation and the saliency information of the blocks. Wang, et al. [33] proposed an adaptive rate compressive sensing method by considering the statistical data analysis for the sparsity calculation. The performance of the method is better, but statistical data analysis increases the execution time and power [34]. Kazemi, et al. [35] proposed a multi focus based image fusion technique by using the adaptive sampling rate. The adaptivity of the block is decided by using textural information. Multi focus fusion approach of images increases the complexity of the method [36].

Most of the methods found in the literature have considered only single feature based approach for the adaptive sampling measurement and only few have considered dual feature based approach, some have experimented on gray images, some have the limitation of higher energy consumption and some have the limitation of higher delay and power requirements [34]. Moreover, most of the methods are non-automatic sampling allocation schemes except the fuzzy based approach.

Therefore, motivated by the state of the requirements and advantages of fuzzy based approach we have designed a fuzzy based ABCS model. Towards this goal we have proposed a novel fuzzy rule based approach for finding the adaptive sampling value selection by using Mamdani fuzzy rule approach. Because of which the sampling rate allocation is completely automatic. Since the proposed work considers two features, it can be better capture the image features for finding the adaptive sampling value.

The contribution of the paper are as follows:

- A novel fuzzy rule based compressive sensing technique for WSN application.
- An automatic threshold generation technique for adaptive sampling by considering two important features.
- Probability based saliency map detection
- Simple provision for handling oversampling cases.

The remainder of this paper are arranged as follows. Section 3 focusses on the proposed method in detail, Section 4 deals with the experiments and result analysis and finally Section 5 concludes the paper.

3. Proposed Method

In this section we have described about proposed fuzzy logic based adaptive sampling rate generation system by considering two important features i.e., edge and saliency information of the block). The proposed method is divided into 4 different stages. The different stages are as in Section 3.1. Block selection and Feature Extraction, Section 3.2. Adaptive sampling phase, Section 3.3. CS measurement phase, Section 3.4. Reconstruction phase. The architecture diagram of the proposed work flow is shown in the Figure 1. The detailed description of the individual stages are described in the following subsection.
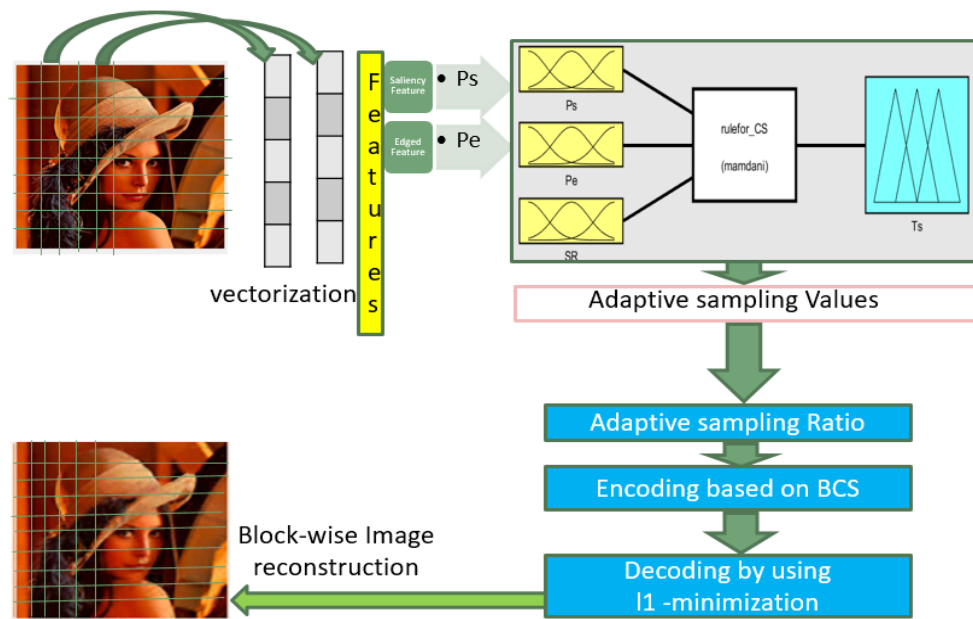
Figure 1. The Proposed Model.

3.1. Block Selection and Feature Extraction

Literature review revealed that the block-based processing for measuring matrix selection has the advantage of less execution time and lower memory requirement in contrast to the traditional CS. However, selection of block size is the key component in BCS approach. The size of the block not only decides the sampling rate and the measuring matrix but also improves the reconstructed image quality. Again, assigning the fixed measuring matrix or the sampling ratio to all the blocks without consideration of different feature content is not an optimal solution. Some image blocks may contain more crucial information while others may not. Therefore, to achieve an effective compression, adaptive sampling rate allocation is highly preferable.

With the aim of maintaining the quality of reconstruction, we have considered two main features i.e., edge and the saliency of the blocks. In this work, the adaptiveness of sampling ratio is decided based on the combination of the edge features and the salient feature data of the block. In this subsection, we primarily discuss about block size selection and suitable feature extraction. Neither a very small size nor a very large size of the block is suitable for optimum feature extraction. Here, the image is divided into 16×16 or 32×32, equal sized non overlapping blocks for feature extraction.

3.1.1. Saliency Detection

The image has been considered as a combination of the different saliency information. Here the saliency map detection is based on the high probability pixels of an image. In this method we have considered the histogram of the image, which gives idea about the probability of occurrence of the image pixels. From the probability information based on histogram data the high probability pixels are obtained as follows.

The threshold value t_1 detection in (1) is based on the highest probability value of an image pixel $I(x, y)$, which gives an ideal bench mark for the high probability pixel occurrence criteria.

$$t_1 = \frac{\max(\text{Probability of } all \text{ pixel})}{2} \tag{1}$$

$$y_1(x1) : \text{ Set of high probability pixels denoted as}$$
$$y_1(x1) \in \{P(x,y) \geq t_1 \tag{2}$$

$P(x, y)$: denotes Probability of a pixel $I(x, y)$ at location (x, y),

Contrast values of the high probability pixels, which are obtained by using the global contrast method are calculated by using (3)

$$D(x1, x1 \in N_1) = \sum_{x,y=1}^{i,j} abs(y1(x1) - I(x,y)) \tag{3}$$

where, $I(x,y)$ is the image pixel value at location (x,y), N_1 is the total number of pixels in $y1$.

The threshold value is obtained based on the sum of average of all contrast values depending upon the number of high probability pixel values in an image. The saliency can be detected based on the threshold as given in (4)

$$Ts = \frac{\sum_{i=1}^{N_1} D(x1_i)}{N_1} \tag{4}$$

The saliency map $(Smap(x,y))$ is obtained using (5)

$$Smap(x,y) = \begin{pmatrix} 1 & D(x1) > Ts \\ 0 & otherwise \end{pmatrix} \tag{5}$$

By counting the number of $1's$ the block wise saliency percentage (P_s) is obtained as given in (6)

$$P_s(\%) = \frac{\text{Total count of } 1}{B \times B} \times 100 \tag{6}$$

where, B is size of image block.

3.1.2. Edge Detection

The edge map of the image is obtained by Canny Edge detection algorithm [37]. Canny edge detection algorithm proceeds through a number of stages to get wide range of edges in an optimal way. The first stage of the algorithm is primarily for smoothening of images, as it reduces the noise level by using the Gaussian filter. In the second stage, the intensity of gradient of the pixel values and the edge thinning technique has been applied to prevent from maximum suppression. Edge map is obtained by double thresholding and connectivity analysis. The edge map is divided into non-overlapping blocks of size $B \times B$. In each block the percentage of $1's$ denoted as P_e is evaluated as given in (7)

$$P_e(\%) = \frac{\text{Total count of } 1}{B \times B} \times 100 \tag{7}$$

The proposed method developed an automatic sampling rate allocation by considering dual feature based fuzzy logic.

For the visual reference saliency map and the edge map of Lena image are shown in Figure 2. The evaluation of saliency feature (P_s) and edge feature (P_s) of the block was done from the saliency map and the edge map as shown in Figure 1. After evaluation of the (P_s) and (P_e) the adaptive sampling of the block was carried out by fuzzy rule based approach, using fuzzy inferencing system described in next subsection.
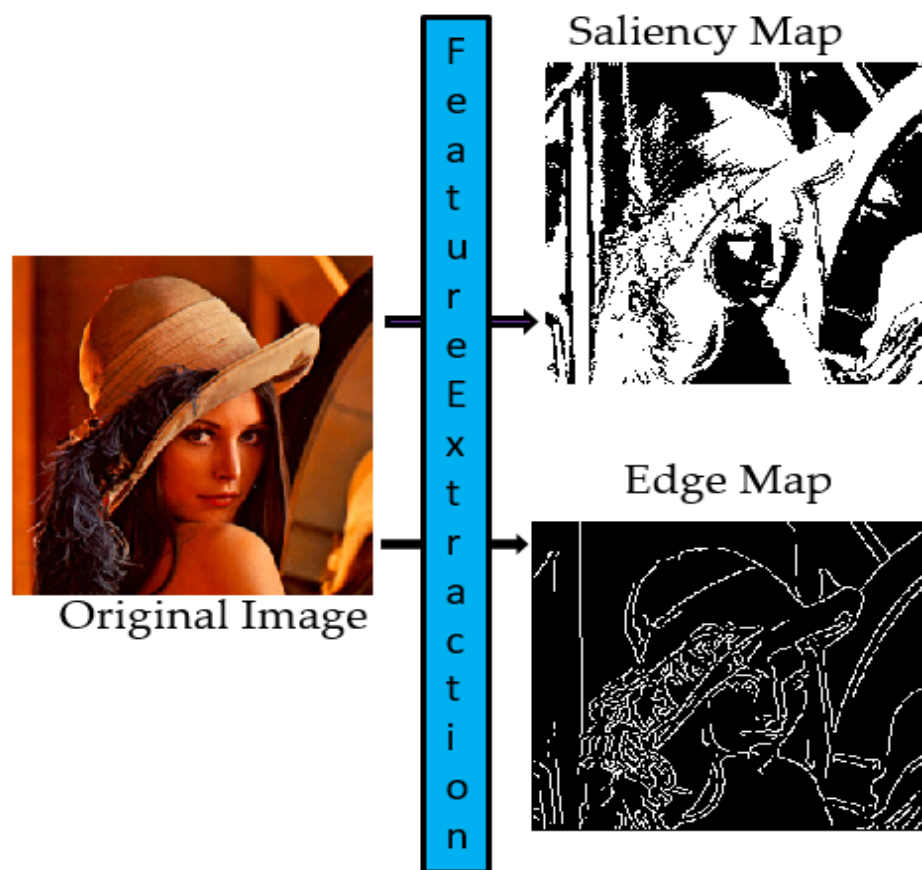
Figure 2. Saliency and Edge Map Representation.
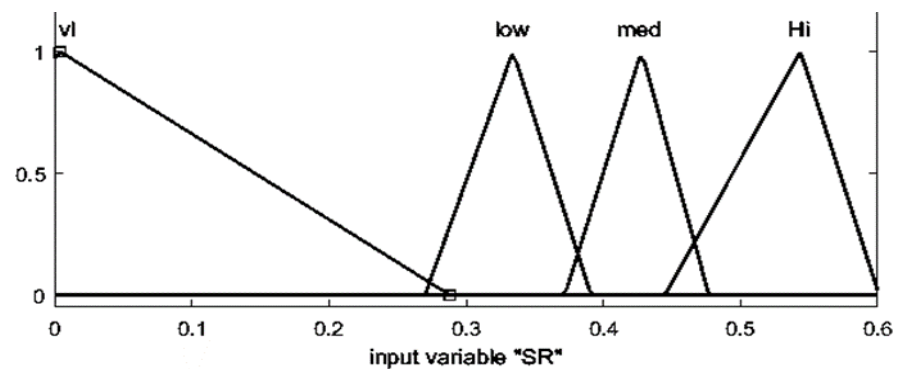
3.2. Adaptive Sampling Phase

In this phase, a feature based adaptive allocation of the sampling rate has been carried out. The adaptive sampling rate allocation was done using fuzzy logic system. This phase is having different decision sub-stages such as designing of fuzzy logic system, adaptive sampling rate allocation by using fuzzy rules, and over sampling correction.

3.2.1. Fuzzy Logic System

L. Zadeh has developed fuzzy logic system, which is a convenient technique in improving the decision making in resource constraint networks i.e., WSN due to its conservation of the resources and operative performance. FLS provide much intelligent solution in the regulator problems by imitating the human thought process. As shown below the FLS has four main components; those are fuzzifier, an inference engine, fuzzy rules, and a defuzzifier. In the fuzzification process, the fuzzifier converts the crisps data into fuzzy sets (linguistic terms are low, medium, high etc.) by considering a membership function. The membership function map the non-fuzzy input into the fuzzy linguistic terms and vice-versa. This process enables the knowledge of the linguistic terms. So many different memberships functions have been developed and deployed in the literature include triangular, trapezoidal, Gaussian, piecewise linear and singleton function. The choice of the membership function has done based on their experience and assessment of the researcher. The membership functions are useful in both the fuzzification and defuzzification process. Fuzzification is followed by fuzzy inferencing process via fuzzy if-then rule base with condition and conclusions. FLS gives the defuzzified membership function as output. Defuzzification process gives the crisp output.

3.2.2. Adaptive Sampling Rate Allocation by Using Fuzzy Rules

In this work a fuzzy rule-based approach has been applied for deciding adaptive sampling of the blocks in an automatic way. The primary motivation to design fuzzy rule based approach for deciding adaptive sampling value is to make the process fully automatic. In this regard, the authors took the advantage of the feature content of each block and the sampling ratio (SR) to decide the adaptive sampling value of the blocks via fuzzy rule-based approach. The feature content of the blocks are captured by the saliency percentage (P_s) and the edge percentage (P_e) of the blocks as described in Sections 3.1.1 and 3.1.2 respectively. Our proposed FLS has three inputs and one output as illustrated in Figure 3. The fuzzy rules are created by carrying out number of experiments on different images. The fuzzy rules have been framed and put in a tabular form in Table 1. While designing the fuzzy rules, care has been taken to maintain the minimum reconstruction quality of the blocks by applying a fixed sampling value. Therefore, irrespective of the feature content of the blocks, a minimum amount of sampling ratio has been assigned to avoid the blocking artifacts. The details of the mamdani based Fuzzy rules are given in Table 1 using various linguistic variables for all inputs and outputs. The triangular and trapezoidal membership functions are studied for representation of the linguistic variables for input and output and the best one is selected. Various possible combination of rules have been exercised and 65 rules have generated and out of those rule 40 basic rules are shown in Table 1. The range of the values of the each and every graph is decided after carrying number of tests upon the image dataset. The proposed fuzzy rule-based approach is well capable to reduce the computation burden by using FLS design. The output value of the FLS is decided by considering the saliency, edge percentage and the sampling ratio.
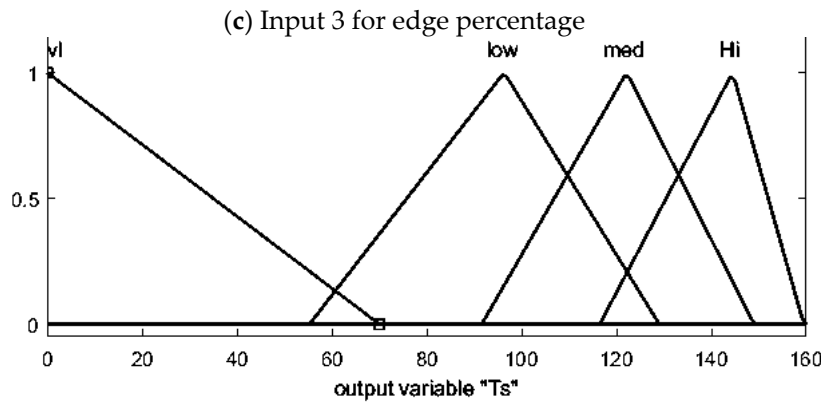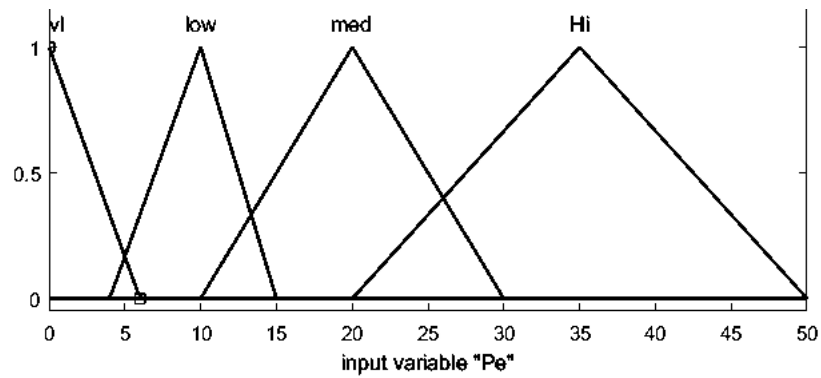

(**a**) Input 1 for sampling rate
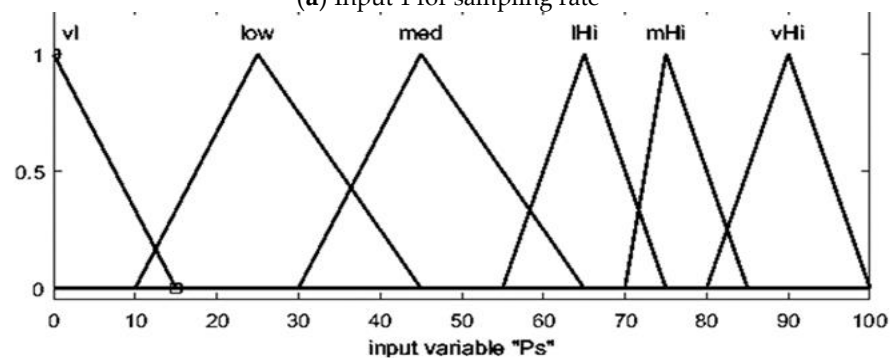
(**b**) Input 2 for saliency percentage

Figure 3. *Cont.*

(**c**) Input 3 for edge percentage

(**d**) Output for adaptive sampling: threshold

Figure 3. Graphical representation of Input and Output membership function.

Table 1. Illustration of the Fuzzy Rules.

| | Fuzzy Rules | | |
Sampling Rate	Saliency Percentage (P_s)	Edge Percentage (P_e)	Adaptive Sampling Values (Th)
Hi	Vl	Vl	Low
Hi	Vl	Med	Low
Hi	Vl	Low	Low
Hi	Vl	Hi	Med
Hi	Low	Low	Med
Hi	Low	Hi	Med
Hi	Low	Med	Med
Hi	Low	Vl	Med
Hi	Hi-Med	Med	Med
Hi	Hi-Med	Low	Med
Hi	Hi-Med	Hi	Hi
Hi	Hi-Med	Vl	Med
Hi	Low-Med	Hi	Med
Hi	Low-Med	Low	Med
Hi	Med-Hi	Vl	Med
Hi	Med-Hi	Med	Hi
Hi	Med-Hi	Low	Med
Med	Vl	Vl	Vl
Med	Vl	Med	Vl
Med	Vl	Low	Vl
Med	Vl	Hi	Low

Table 1. *Cont.*

| Sampling Rate | Fuzzy Rules | | Adaptive Sampling Values (Th) |
	Saliency Percentage (P_s)	Edge Percentage (P_e)	
Med	Low	Low	Low
Med	Low	Hi	Med
Med	Low	Med	Low
Med	Low	Vl	Low
Med	Hi-Med	Med	Low
Med	Hi-Med	Low	Low
Med	Hi-Med	Hi	Med
Med	Hi-Med	Vl	Low
Med	Low-Med	Hi	Med
Med	Low-Med	Low	Low
Low	Hi-Med	Vl	Low
Low	Low-Med	Hi	Low
Low	Low-Med	Low	Low
Low	Med-Hi	Vl	Low
Low	Med-Hi	Med	Low
Low	Med-Hi	Low	Low
Low	Med-Hi	Hi	Low
Low	Low-Hi	Vl	Vl
Low	Low-Hi	Low	Vl
Low	Low-Hi	Hi	Low

Vl = Very low, Med = Medium, Hi = High, Med-Hi = Medium High, Low-Med = Low Medium, Hi-Med = High medium.

3.2.3. Over Sampling Corrections

The output of the FLS is optimum. However, in some cases the adaptive sampling value exceeds the block size, where the block is processed as an uncompressed block. This condition is known as oversampling of the blocks. Oversampling can lead to lower performance of the compression algorithm therefore it must be avoided. To avoid this condition, the oversampling of the blocks is checked after generation of the output of the FLS. In case the block suffers from oversampling a corrective measure, need to be taken. To deal with the oversampling, first the oversampled value is obtained by subtracting the block size from the adaptive measured sampling data. Subsequently the oversampled values are distributed among all the non-over sampled blocks as per an algorithm discussed below.

Let *Bs*: denotes the block size, Am denotes adaptively measured sampling value, *Nb*: denotes total number of blocks, *As*: denotes adaptive sampling, *Os* denotes over sampling value and n denotes as the number of non over sampling blocks. Using these notations the algorithm to handle the oversampling of the blocks is given as follows in Algorithm 1.

Algorithm 1: Over Sampling Corrections

For $i = 1 : Nb$
  $Os = 0; n = 0;$
If $(Am(i) >= Bs)$
over sampled block
  Then $Os(i) = Am(i) - Bs;$
   $As(i) = Am(i) - Os(i);$*
$Os = Os(i) + Os;$
$n = n + 1;$
Else
# *Non oversampled block*
  $As(i) = Am(i) + Os/n;$
End if
End for

3.3. Compressive Sensing Measurement Phase

In the proposed approach, the adaptive sampling is followed by compressive sensing for the encoding and decoding of the image data. In this section a detailed description of the CS and BCS have been given. According to conventional CS theory an image can be reconstruct from few linear measurements if the signal is sparse enough. A signal is sparse in the transform domain if most of the elements are zero and nearly sparse if prominent feature portions are zero or nearly zero. The basic idea in the CS is that a signal can be recovered from very less decoded information. Suppose, x represents a signal of length L and K sparse in the transform domain, ψ represents the transform basis of x of size $L \times L$. θ gives the transform domain representation of the x having only K coefficients. x is represented as $x = \theta\psi$. The linear transform process of getting the value of y (size $M < L$) from x is known as the CS sampling. The linear equation illustrating CS sampling is given in (8).

$$y_i = \Phi x = \Phi \theta \psi \qquad (8)$$

Here, Φ: represents random measuring matrix of size $M \times L$. Then x can be recovered completely by considering $M = O(K \log \frac{L}{K})$ measurements and by solving the convex optimization problem. To make the signal reconstruction easier x represented in the l1 norm form as in (11).

$$x = \operatorname{argmin} \min_{x:y=\phi x} \|x\|_1 \qquad (9)$$

The 2D image signal has converted into the 1D signal, followed by conversion into sparse signal by using transforms such as DCT [Discrete Cosine Transform] or DWT [Discrete wavelet Transform]. Further, the l1-minimization process for the 1-D signal reconstruction.

Block Compressive Sensing Method for Image Compression

The CS based approach for compressive sensing is very impressive in terms of performance. However, the major issue is pertaining to the reconstruction of the large sized image with lower computational complexity. Moreover, handling the entire image data, requires large size measuring matrix or sampling matrix which leads to undesirable increase in the complexity and larger storage requirement. To mitigate these issues BCS scheme has been proposed.

In BCS, image is divided into $B \times B$ non-overlapping blocks and each block is then considered as a 2D signal. A fixed sampling rate r is applied to the image block x_i and the sampled value acquired denoted as y_i are related as given in (10).

$$y_i = \Phi^{(B)} x_i = \Phi^{(B)} \psi^{(B)} X_i \qquad (10)$$

Here the $\Phi^{(B)} = n_B \times B^2$ represents the measuring matrix of the image block, which is constructed by selecting $n_B = (r \times B^2)$, rows from a matrix of size $(B^2 \times B^2)$ and the transform matrix $\psi^{(B)}$ of size $(B^2 \times B^2)$. Both the transform matrix and the sparse vector will form $x_i = \psi^{(B)} X_i$. The computation of sampling matrix for the image block is space and time saving process than the entire image sampling matrix calculation. The encoded signal is transmitted through the transmitter by having all the adaptive sampling information.

3.4. Reconstruction Phase [10]

In this phase the decoding of the compressed data is carried out. For the image reconstruction many different techniques can be found in the literature. However, l1-minimization based technique for the image reconstruction is preferable owing to its higher accuracy [4]. The BCS-SPL approach has attracted attention of many researchers due to incomplete data handling and lower reconstruction artifacts, which is suitable for real time application. In this work, we have built a fuzzy rule based adaptive sampling design approach for BCS-SPL algorithm.

4. Experimental Design and Result Analysis

To evaluate the proposed method we have experimented on four different types of dataset. In the first phase we have considered 6 different.tiff standard colour images i.e., Lena, Zelda, Couple, House, Baboon, Peppers image. In the second phase, we have considered Kodak dataset [38] comprising of 25 colour images. In the third phase, we have considered the low resolution real life CCTV images [39] collected from the National park surveillance system. To evaluate the performance of the proposed method for different resolution of the images here we have considered some high resolution images from the Set5 dataset [40]. All the images considered above are resized to a size of 256×256. To evaluate the performance of the method both subjective and objective evaluation has been performed. The subjective analysis has been done based on the perceptual view whereas, objective analysis has been done based on suitable performance parameters evaluation such as PSNR (Peak Signal to Noise Ratio) and Structural similarity Index matrix measurement (SSIM) [41]. All simulations are carried out considering non overlapping blocks of size 16×16. The objective evaluation of the proposed method has been given in Table 2, based on PSNR [13] and SSIM [41] comparison of different state of the art methods such as BCS-SPL [11], ENT-ABCS [6], STD_BCS-SPL [26] and EABCS [31] with proposed FABCS approach. Although different reconstruction approaches can be found in the literature [10,12,31], but l1-minimization based reconstruction approach has reduced blocking artifacts with superior reconstruction image quality [10]. Therefore, to do a fair comparison l1 minimization based reconstruction approach is applied for all the methods.

The subjective evaluation is made based on the visual quality of the reconstructed image. For all the considered methods the reconstructed images of standard dataset are shown in Figure 4. Figure 4a illustrates the original images of Lena, Zelda, Couple, Baboon and House. Figure 4b–f indicate the reconstructed images using BCS-SPL, STD-BCS-SPL, ENT-ABCS, EABCS and FABCS at a SR of 0.5. From Figure 4 it is found that the perceptual quality of the proposed FABCS method is the best among all the approaches considered for evaluation. Out of all the methods considered for evaluation, the BCS-SPL [9] method is based on a fixed compression rate for all the blocks of image. Which is having a restriction to enhance the reconstruction quality based on block feature content. The STD-BCS-SPL [26] framework considered the standard deviation as a threshold to extract the block wise information content. The higher the information content of the block, the lesser is the sampling ratio and the lower the information content of the block, higher is the sampling ratio. The STD-BCS-SPL method is applicable for restricted WSN application [26]. It has lower computational complexity with better-reconstruction quality of the image. However, Due to the manual calculation the sampling rate allocation is time consuming. In ENT-ABCS [6] method, the entropy of the block was selected to generate the threshold for deciding the adaptive sampling. It relied only on one feature for finding the block adaptivity. In the EABCS method [30] the energy of the block was considered for the adaptive sampling rate selection suitable for IoUT (under water based Internet on things) application. All the state of art methods discussed above have considered only single feature for deciding adaptive sampling. In the proposed approach the dual feature combination can capture even the finer details of the block. The bold faced value in each row of Table 2 indicates the highest value of the performance parameters of corresponding image. It is observed from Table 2 that the proposed method out performed all the other existing methods based on average PSNR and SSIM values for all the images considered for evaluation. Moreover, the fuzzy rule-based evaluation of the adaptive sampling is well capable to provide an automatic image adaptive sampling ratio generation to reduce the computation with better PSNR and SSIM values than the state-of-the-art methods as depicted in the Table 2.

Figure 4. Reconstructed Lena, Zelda, Couple, Baboon and House image by using different ABCS methods (**a**) original image, (**b**) BCS-SPL, (**c**) STD-BCS-SPL, (**d**) ENT-ABCS, (**e**) EABCS, (**f**) FABC at 0.5 sampling rate.

Table 2. Performance comparison of different state of the art methods based on PSNR and SSIM parameters for different state of the art methods at 0.3, 0.4, and 0.5 SR.

Images		BCS-SPL [11]		ENT-ABCS [6]		STD_BCS-SPL [26]		EABCS [31]		FABCS	
		PSNR	SSIM	PSNR	SSIM	PSNR	SSIM	PSNR	SSIM	PSNR	SSIM
0.3	Zelda	30	0.751	32.2	0.811	32.3	0.838	32	0.75	**33.41**	**0.8565**
	Couple	31	0.742	32.6	0.797	32.8	0.809	32.3	0.77	**32.88**	**0.8345**
	House	30	0.735	32.2	0.756	32.5	0.764	32	0.74	**32.7**	**0.8125**
	Baboon	25	0.574	28.9	0.563	28.8	0.522	28.9	0.55	**30.56**	**0.6788**
	Lena	29	0.812	31.9	0.778	31	0.75	31.3	0.75	**33.41**	**0.8342**
	Average	28.9	0.723	31.56	0.741	31.49	0.7366	31.28	0.7132	**32.792**	**0.8031**
0.4	Zelda	31	0.861	32.9	0.846	33.4	0.871	32.8	0.8	**33.89**	**0.8641**
	Couple	32	0.855	33.4	0.833	33.7	0.8464	33	0.81	**34.47**	**0.8568**
	House	32	0.822	32.9	0.784	33.9	0.8441	32.6	0.78	**34.34**	**0.8588**
	Baboon	29	0.626	29.3	0.673	30.3	0.6987	29.3	0.57	**31.03**	**0.7837**
	Lena	31	0.841	32.6	0.817	33	0.8417	32	0.79	**34.03**	**0.8723**
	Average	30.8	0.801	32.24	0.7907	32.8	0.82038	31.94	0.7496	**33.552**	**0.8471**
0.5	Zelda	31	0.889	33.5	0.867	34	0.886	33.4	0.82	**34.99**	**0.9029**
	Couple	33	0.883	34	0.856	34.4	0.8693	33.4	0.83	**35.52**	**0.9152**
	House	32	0.85	33.5	0.807	34.5	0.8711	33.1	0.81	**35.11**	**0.8704**
	Baboon	31	0.756	30.5	0.717	31	0.7412	29.6	0.61	**31.23**	**0.8032**
	Lena	32	0.881	33.2	0.844	33.6	0.8642	32.7	0.82	**34.49**	**0.8881**
	Average	32	0.852	32.93	0.818	33.5	0.846	32.4	0.778	**34.27**	**0.876**

The second experiment was done for the real-life low resolution original CCTV images [39]. The evaluation of the FABCS performance using CCTV images are presented in the Table 3 and compared with four state of the art methods. Figure 5 shows the reconstructed CCTV images by different methods. It is observed from Figure 5 that the dual features consideration of the proposed approach is well capable to maintain the reconstruction quality even for the low resolution CCTV images. Dual feature selection scheme ensures better feature extraction and hence the higher PSNR and SSIM values as compared to the state of the art methods. Table 3 represents the comparison of the state-of-the-art methods with proposed FABCS method by using the real life CCTV image from a National Park [36]. The bold faced value in each of Table 3 indicates the highest values of the performance parameters of corresponding image. The Table 3 shows that the proposed method has higher PSNR and SSIM values than the other methods. The SSIM and the PSNR values of the FABCS indicate that it has restored more features during reconstruction phase than other state of the art approaches. The subjective evaluation is made based on the visual quality of the reconstructed image and shown in Figures 4 and 5 respectively.
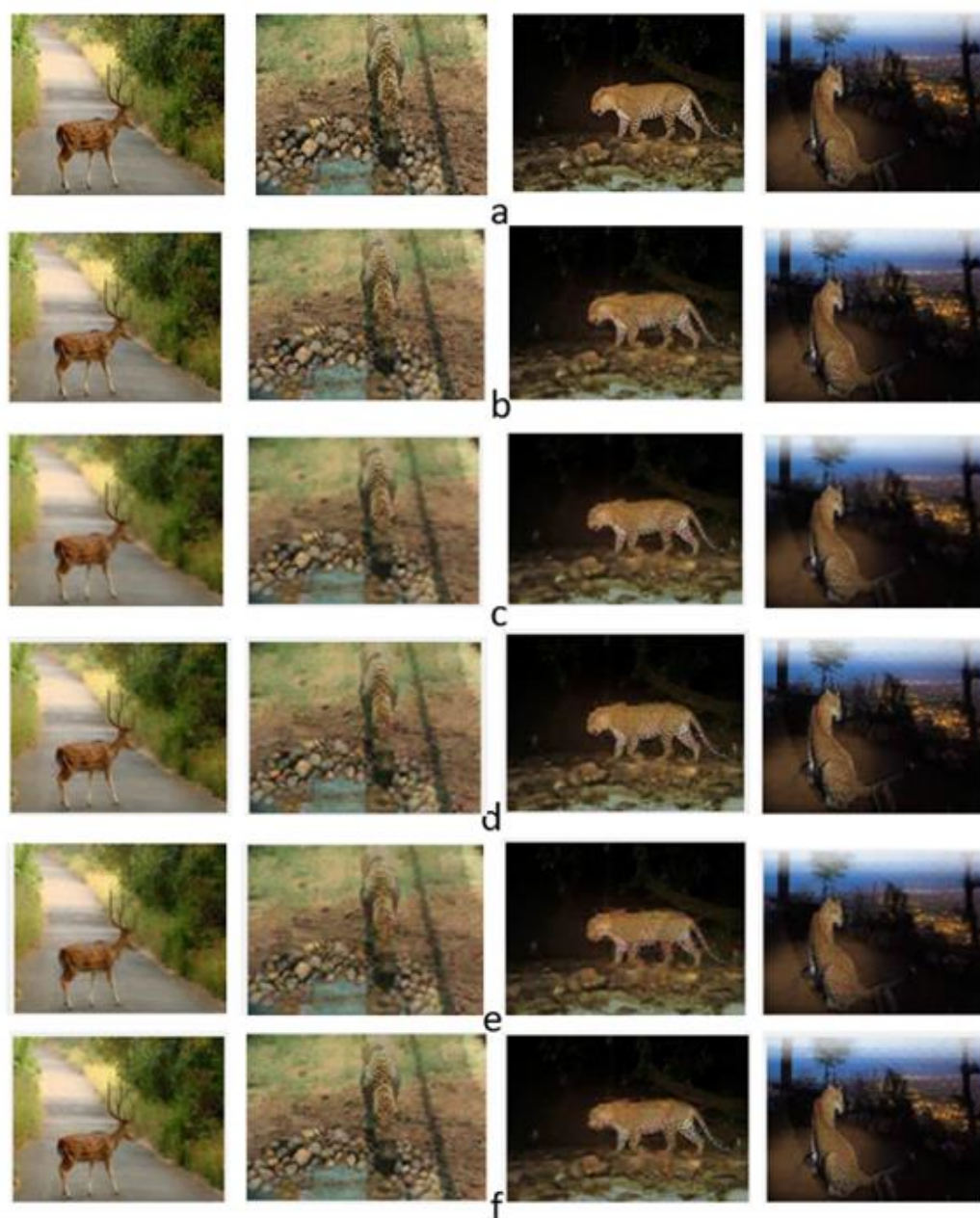
Figure 5. Reconstructed Deer, Leopards images at SR of 0.5 for different methods. (**a**) Original image, (**b**) BCS-SPL, (**c**) STD-BCS-SPL, (**d**) ENT-ABCS, (**e**) EABCS, (**f**) FABCS.

The proposed FABCS method outperformed the other ABCS methods in terms of both subjective and objective evaluation metrics. In the proposed method the adaptive sampling allocation has been done by using the Fuzzy Logic System. Further experiments were carried out to study the effect of variation of SR values on the performance parameter PSNR and SSIM and placed in Figure 6. Figure 6a–e illustrate the statistical representation of average PSNR and SSIM values of the FABCS method with other state of the art methods at SR value of 0.3, 0.4 and 0.5 respectively for standard data set images (i.e., Lena, Zelda, Couple, Baboon and House).

Table 3. Performance comparison of the state of the art methods at 0.5 SR on CCTV images.

Images	BCS-SPL [11]		ENT-ABCS [6]		STD-ABCS [26]		EABCS [31]		FABCS	
	PSNR	SSIM	PSNR	SSIM	PSNR	SSIM	PSNR	SSIM	PSNR	SSIM
Deer	31.84	0.82	32	0.85	32.7	0.86	31.99	0.85	**33.05**	**0.9**
Leopard1	27.89	0.708	29.63	0.78	29.6	0.789	30.65	0.812	**31.92**	**0.83**
Leopard2	31.32	0.821	32.38	0.81	33.23	0.84	30.24	0.828	**33.68**	**0.869**
Leopard3	32.13	0.838	31.71	0.83	33.44	0.85	31.23	0.806	**33.82**	**0.878**
Leopard4	31.42	0.827	32.44	0.85	32.58	0.842	32.1	0.85	**32.73**	**0.85**
Leopard5	30.56	0.81	32.56	0.85	32.82	0.865	29.84	0.795	**33.18**	**0.86**
Average	30.86	0.8	32	0.82	32.01	0.84	31.01	0.83	**33.06**	**0.86**

From the image wise analysis it is observed from Figure 6 that the baboon image has the lowest SSIM and PSNR values due to the less sharp features. Couple, House and Lena have SSIM and PSNR values close to each other. The Zelda has the highest SSIM and PSNR values among all the five images as the image has high information content. From the image wise performance analysis, it can be concluded that the proposed method outperformed the state of the art methods. Figure 6g,h illustrate the average PSNR and SSIM comparison of different state of the art methods with FABCS method at 0.3, 0.4 and 0.5 sampling rates for standard dataset images. Figure 6i,j illustrate the average PSNR and SSIM comparison of different state of the art methods with FABCS method at 0.3, 0.4 and 0.5 sampling rates for Kodak dataset.
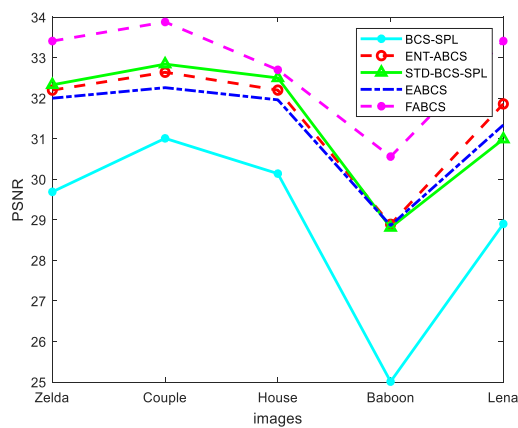
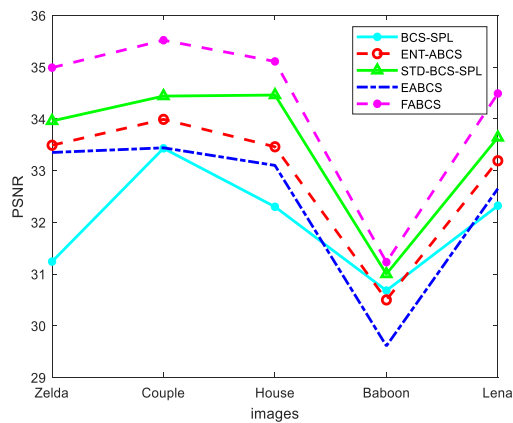(**a**) PSNR at 0.3 SR
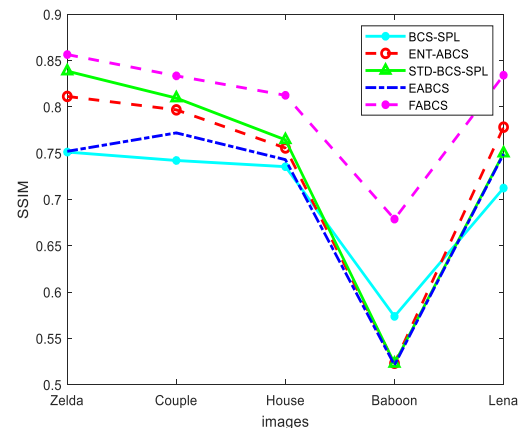
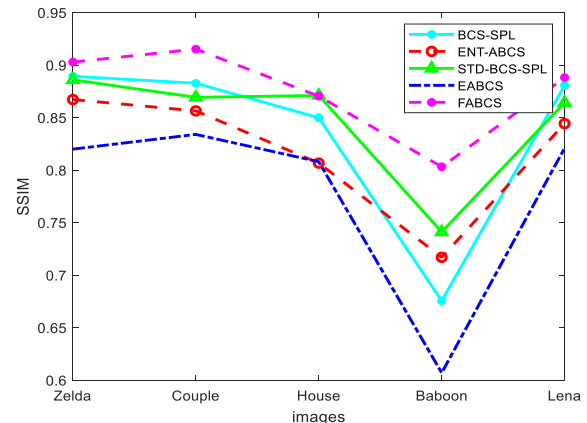(**b**) SSIM at 0.3 SR
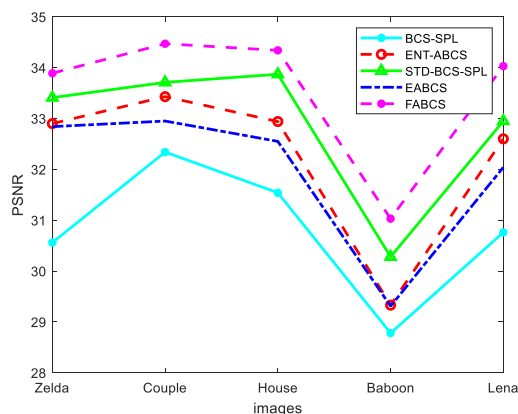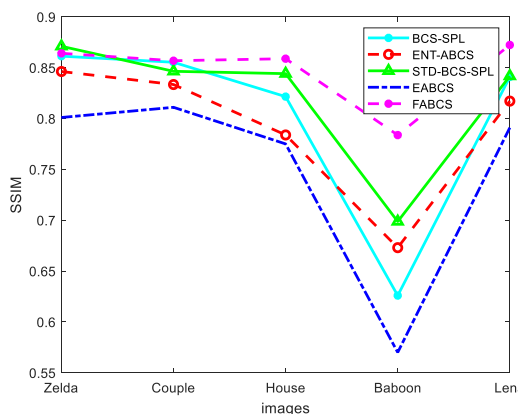
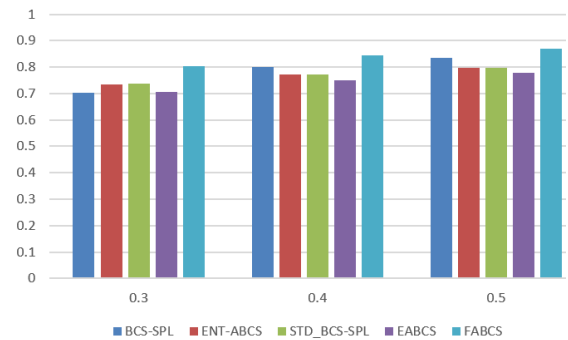(**c**) PSNR at 0.4 SR

(**d**) SSIM at 0.4 SR

Figure 6. *Cont.*
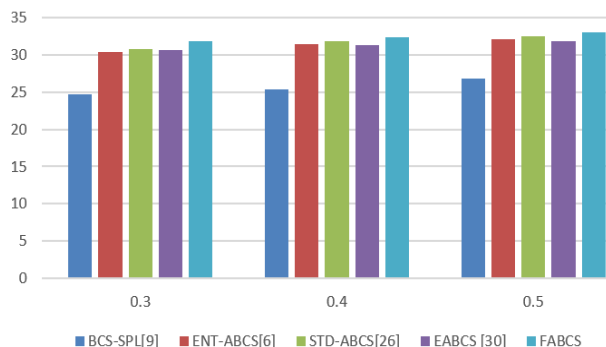
(**e**) PSNR at 0.5SR

(**f**) SSIM at 0.5 SR
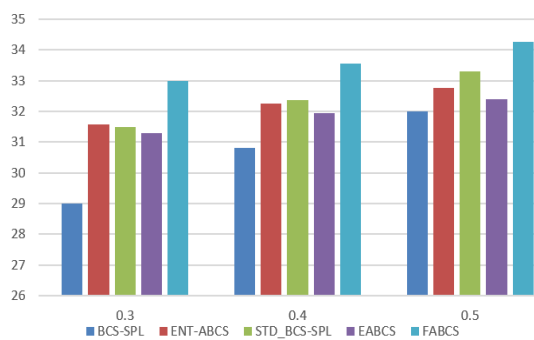
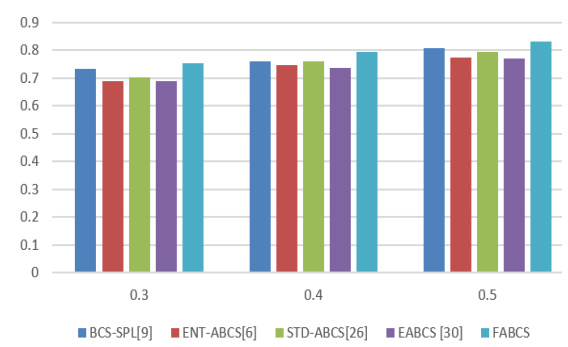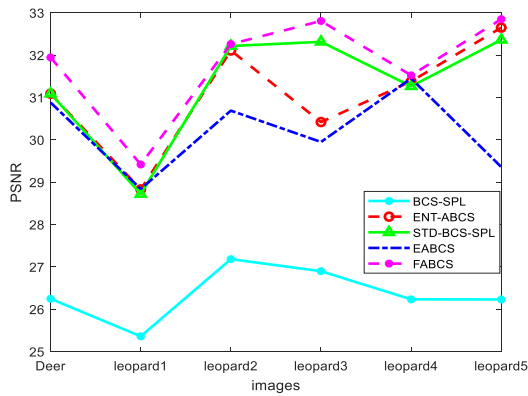(**g**) Average PSNR

(**h**) Average SSIM

(**i**) Average PSNR for the Kodak dataset

(**j**) Average SSIM for the Kodak dataset

Figure 6. (**a**–**f**) Performance comparison of different algorithms on Standard images and (**g**,**h**), (**i**,**j**) average PSNR and SSIM for standard images and Kodak dataset images.

To check the performance of the algorithm in the real time image some CCTV images have been taken into consideration. The performance comparison has illustrated in Figure 7. The Figure 7a–f illustrate the detail analysis of the proposed FABCS method over the state of the art methods for CCTV images for different sampling rates at 0.3, 0.4, and 0.5 respectively. The average PSNR and SSIM value are shown in Figure 7g,h which indicate that the proposed FABCS method has the highest PSNR and SSIM than all the state of the art methods by using real time images.
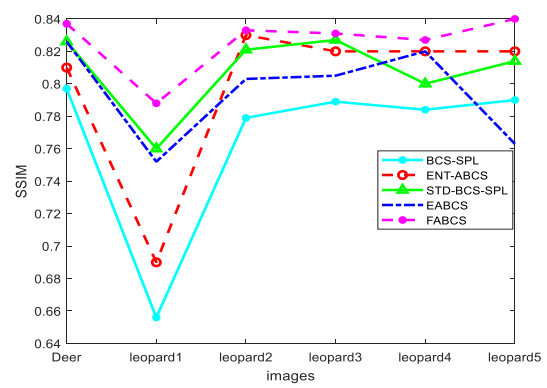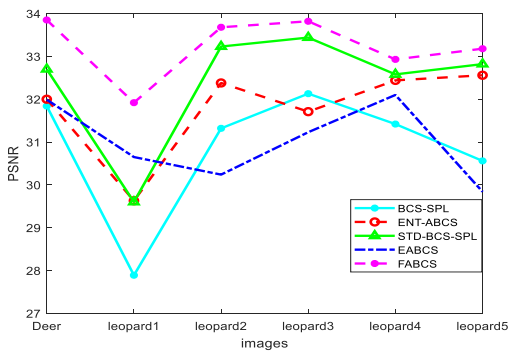
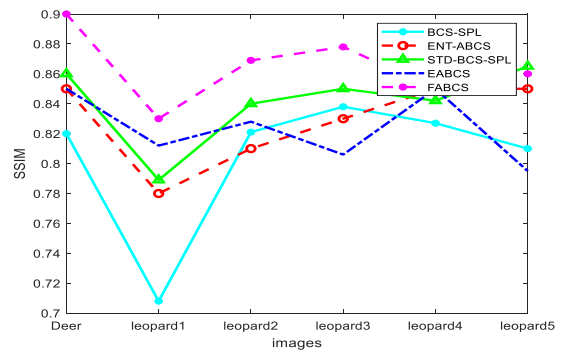(**a**) PSNR at 0.3 SR
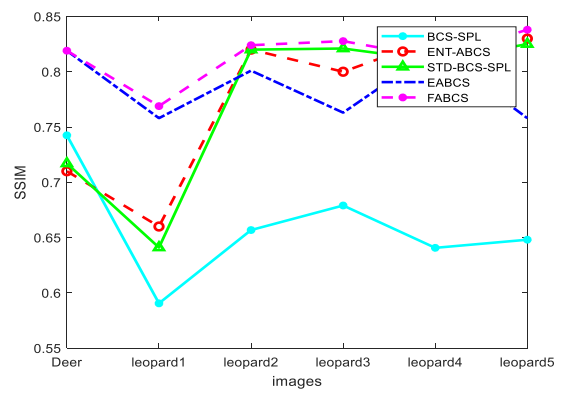
(**b**) SSIM at 0.3 SR
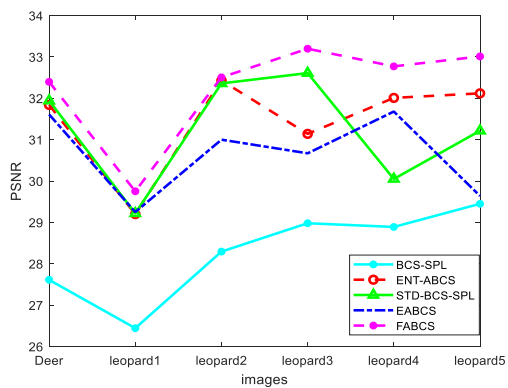
(**c**) PSNR at 0.4 SR

(**d**) SSIM at 0.4 SR

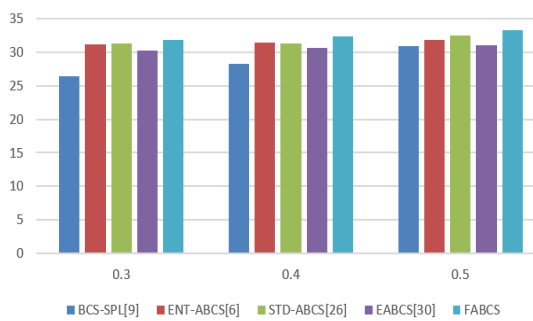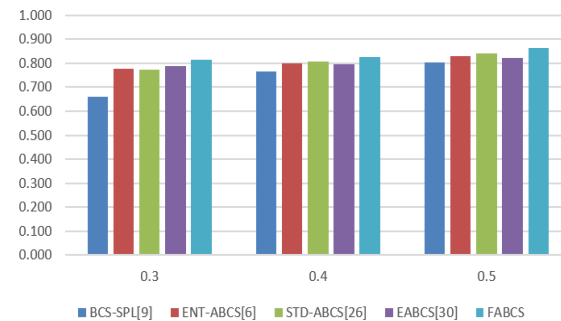(**e**) PSNR at 0.5 SR

(**f**) SSIM at 0.5 SR

(**g**) Average PSNR

(**h**) Average SSIM

Figure 7. Performance comparison of different algorithms on CCTV images based on PSNR and SSIM.

In order to study the performance of the proposed algorithm on high resolution images we have also experimented on Set5 dataset and the results are placed in Figure 8. It is apparent from Figure 8 that FABCS has also performed well for high resolution images in terms of higher PSNR and SSIM values than the state of the art methods.
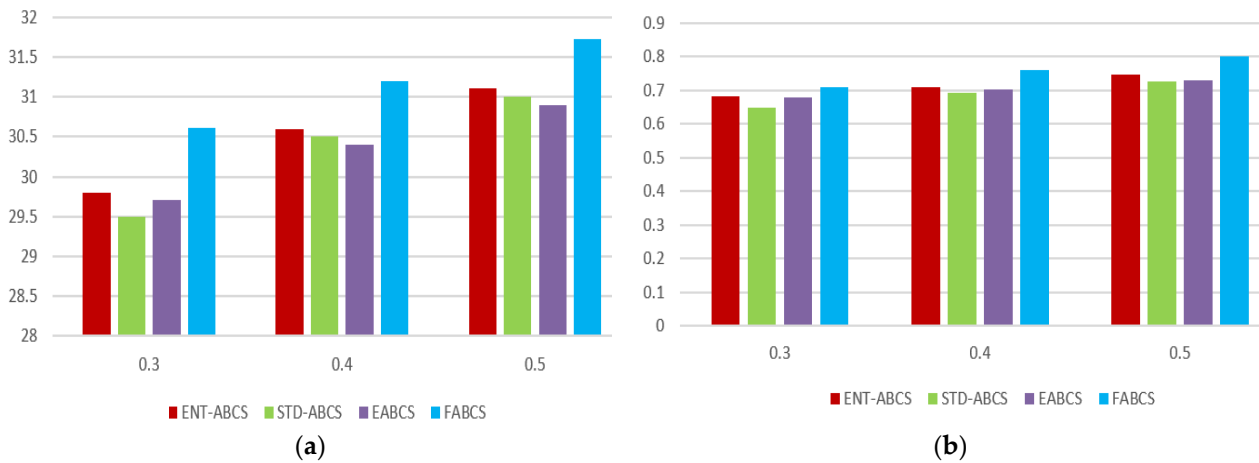

Figure 8. Performance comparison of different algorithms on Set5 Test images based on (**a**) Average PSNR and (**b**) Average SSIM.

Figure 9 shows the performance comparison of the fuzzy based adaptive sampling method with the non-fuzzy based adaptive sampling method. For the comparison purpose we have computed the sampling value of the proposed method with and without fuzzy based approach followed by BCS. The performance is evaluated for standard dataset images and the average value is considered. Average PSNR and SSIM value of the fuzzy based ABCS method is 2% higher than the non-fuzzy based ABCS method. The performance of the fuzzy method is higher due to better and a balanced distribution of the sampling rate allocation for the blocks.
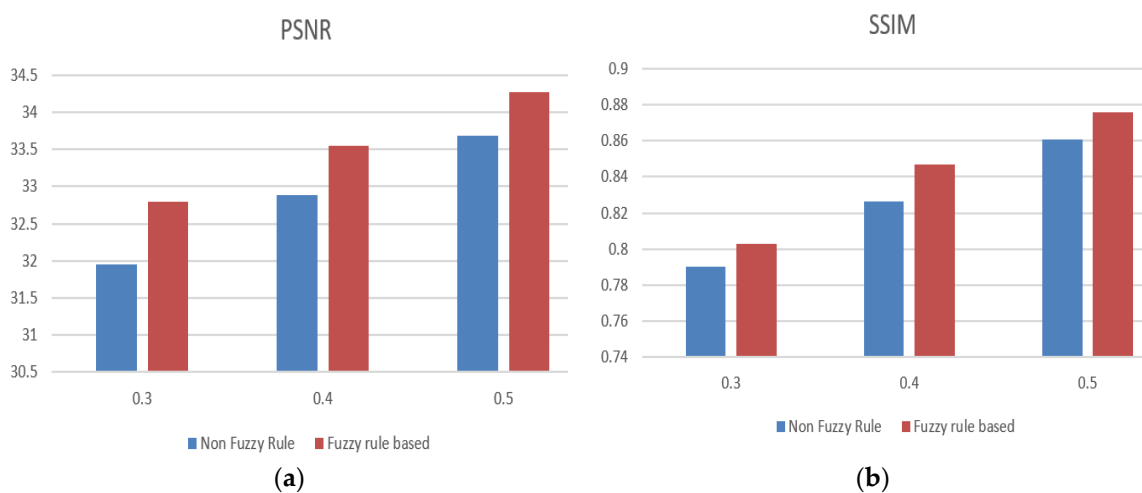

Figure 9. Performance comparison of the Fuzzy and Non fuzzy based approach in terms of (**a**) PSNR and (**b**) SSIM.

We have tested our algorithm performance with the 4 different images data set and the statistical analysis of the PSNR and SSIM evaluation has been depicted in the Figures 6–8. Table 4 shows the comparison of average execution time (ET) of different algorithms for standard images of block size (16×16).

It is evident from Table 4 that the proposed FABCS method has less ET than the BCS_SPL for a block size of 16×16 block size. The FABCS has ET lesser than BCS-SPL [11] and slightly more ET than the other state of art methods, due to consideration of dual features and 65 fuzzy rules for automation of the process.

Table 4. Comparison of the ET of different methods in second.

Methods	BCS-SPL [11]	ENT-ABCS [6]	STD_BCS-SPL [26]	EABCS [31]	FABCS
ET (s)	0.376	0.245	0.26	0.252	0.32

Result analysis shows that the proposed FABCS is efficient in terms of better performance measure parameters. The main attraction is the consideration of dual feature selection to capture the content of the images and simple l1 minimization based image reconstruction approach. The fuzzy based block sampling ratio detection has made the algorithm automatic and more effective. Moreover, the proposed approach is followed by a corrective action which ensured that the algorithm should not over sample the block data.

5. Conclusions

The proposed FABCS method is an efficient approach to give a better alternative solution to deal with the practical problem of the data transmission in a wireless sensor network. The proposed method has reduced the computational burden by introducing the fuzzy based adaptive sampling ratio selection in an automatic way. Dual feature selection for threshold detection ensures minimal data loss. The proposed method performed equally well for all variety of test images including standard dataset image, low resolution CCTV image and high resolution Set5 dataset images. The proposed method achieved an average PSNR of 34.26 and average SSIM if 0.87 standard test images. Similarly, it has achieved an average PSNR of 33.2 and SSIM of 0.865 for CCTV images. However, the proposed method can still be improved by considering other features like colour, texture etc. and optimizing the fuzzy rules.

Author Contributions: Conceptualization, D.N. and T.K.; Methodology, D.N. and S.N.M.; Software, D.N. and T.K.; Validation, T.K.; Formal analysis, K.R. and T.K.; Investigation, S.N.M.; Resources, K.R.; Writing—original draft, D.N.; Writing—review & editing, D.N.; Supervision, K.R. and S.N.M.; Funding acquisition, S.N.M. All authors have read and agreed to the published version of the manuscript.

Conflicts of Interest: The authors declare no conflict of interest.

References

1. Majid, M.; Habib, S.; Javed, A.R.; Rizwan, M.; Srivastava, G.; Gadekallu, T.R.; Lin, J.C.-W. Applications of Wireless Sensor Networks and Internet of Things Frameworks in the Industry Revolution 4.0: A Systematic Literature Review. *Sensors* **2022**, *22*, 2087. [CrossRef]
2. Tavli, B.; Bicakci, K.; Zilan, R.; Barcelo-Ordinas, J.M. A survey of visual sensor network platforms. *Multimedia Tools Appl.* **2011**, *60*, 689–726. [CrossRef]
3. Charalampidis, P.; Fragkiadakis, A.G.; Tragos, E.Z. Rate-Adaptive Compressive Sensing for IoT Applications. In Proceedings of the 2015 IEEE 81st Vehicular Technology Conference (VTC Spring), Glasgow, UK, 11–14 May 2015; pp. 1–5. [CrossRef]
4. Fayed, S.; Youssef, S.M.; El-Helw, A.; Patwary, M.; Moniri, M. Adaptive compressive sensing for target tracking within wireless visual sensor networks-based surveillance applications. *Multimedia Tools Appl.* **2015**, *75*, 6347–6371. [CrossRef]
5. Li, R.; Duan, X.; Li, X.; He, W.; Li, Y. An Energy-Efficient Compressive Image Coding for Green Internet of Things (IoT). *Sensors* **2018**, *18*, 1231. [CrossRef] [PubMed]

6.   Rippel, O.; Bourdev, L. Real-time adaptive image compression. In Proceedings of the 34th International Conference on Machine Learning, Sydney, Australia, 6–11 August 2017; Volume 70, pp. 2922–2930.

7.   Zammit, J.; Wassell, I.J. Adaptive Block Compressive Sensing: Toward a Real-Time and Low-Complexity Implementation. *IEEE Access* **2020**, *8*, 120999–121013. [CrossRef]

8.   Xiao, W.; Wan, N.; Hong, A.; Chen, X. A Fast JPEG Image Compression Algorithm Based on DCT. In Proceedings of the 2020 IEEE International Conference on Smart Cloud (SmartCloud), Washington, DC, USA, 6–8 November 2020; pp. 106–110. [CrossRef]

9.   Gungor, M.A.; Gencol, K. Developing a Compression Procedure based on the Wavelet Denoising and Jpeg2000 Compression. *Optik* **2020**, *218*, 164933. [CrossRef]

10. Donoho, D.L. Compressed sensing. *IEEE Trans. Inf. Theory* **2006**, *52*, 1289–1306. [CrossRef]

11. Gan, L. Block compressed sensing of natural images. In Proceedings of the 2007 15th International Conference on Digital Signal Processing, Cardiff, UK, 1–4 July 2007; pp. 403–406.

12. Monika, R.; Samiappan, D.; Kumar, R. Adaptive block compressed sensing—A technological analysis and survey on challenges, innovation directions and applications. *Multimedia Tools Appl.* **2020**, *80*, 4751–4768. [CrossRef]

13. Zha, Z.; Liu, X.; Zhang, X.; Chen, Y.; Tang, L.; Bai, Y.; Wang, Q.; Shang, Z. Compressed sensing image reconstruction via adaptive sparse nonlocal regularization. *Vis. Comput.* **2016**, *34*, 117–137. [CrossRef]

14. Monika, R.; Dhanalakshmi, S.; Kumar, R.; Narayanamoorthi, R. Coefficient Permuted Adaptive Block Compressed Sensing for Camera Enabled Underwater Wireless Sensor Nodes. *IEEE Sens. J.* **2021**, *22*, 776–784. [CrossRef]

15. Xu, J.; Qiao, Y.; Fu, Z. Adaptive Perceptual Block Compressive Sensing for Image Compression. *IEICE Trans. Inf. Syst.* **2016**, *99*, 1702–1706. [CrossRef]

16. Heng, S.; Aimtongkham, P.; Vo, V.N.; Nguyen, T.G.; So-In, C. Fuzzy Adaptive-Sampling Block Compressed Sensing for Wireless Multimedia Sensor Networks. *Sensors* **2020**, *20*, 6217. [CrossRef]

17. Sun, F.; Xiao, D.; He, W.; Li, R. Adaptive Image Compressive Sensing Using Texture Contrast. *Int. J. Digit. Multimedia Broadcast.* **2017**, *2017*, 3902543. [CrossRef]

18. Gao, X.; Zhang, J.; Che, W.; Fan, X.; Zhao, D. Block-Based Compressive Sensing Coding of Natural Images by Local Structural Measurement Matrix. In Proceedings of the 2015 Data Compression Conference, Snowbird, UT, USA, 7–9 April 2015; pp. 133–142. [CrossRef]

19. Yu, Y.; Wang, B.; Zhang, L. Saliency-Based Compressive Sampling for Image Signals. *IEEE Signal Process. Lett.* **2010**, *17*, 973–976. [CrossRef]

20. Zhang, Z.; Bi, H.; Kong, X.; Li, N.; Lu, D. Adaptive compressed sensing of color images based on salient region detection. *Multimedia Tools Appl.* **2019**, *79*, 14777–14791. [CrossRef]

21. Feng, W.; Zhang, J.; Hu, C.; Wang, Y.; Xiang, Q.; Yan, H. A novel saliency detection method for wild animal monitoring im-ages with WMSN. *J. Sens.* **2018**, *2018*, 3238140. [CrossRef]

22. Liu, W.; Liu, H.; Wang, Y.; Zheng, X.; Zhang, J. A novel extraction method for wildlife monitoring images with wireless mul-timedia sensor networks (WMSNS). *Appl. Sci.* **2019**, *9*, 2276. [CrossRef]

23. Liu, G.; Zheng, X. Fabric defect detection based on information entropy and frequency domain saliency. *Vis. Comput.* **2020**, *37*, 515–528. [CrossRef]

24. Li, R.; Duan, X.; Guo, X.; He, W.; Lv, Y. Adaptive Compressive Sensing of Images Using Spatial Entropy. *Comput. Intell. Neurosci.* **2017**, *2017*, 9059204. [CrossRef]

25. Xin, L.; Junguo, Z.; Chen, C.; Fantao, L. Adaptive sampling rate assignment for block compressed sensing of images using wavelet transform. *Open Cybern. Syst. J.* **2015**, *9*, 683–689. [CrossRef]

26. Zhang, J.; Xiang, Q.; Yin, Y.; Chen, C.; Luo, X. Adaptive compressed sensing for wireless image sensor networks. *Multimedia Tools Appl.* **2016**, *76*, 4227–4242. [CrossRef]

27. Zhao, H.H.; Rosin, P.L.; Lai, Y.-K.; Zheng, J.-H.; Wang, Y.-N. Adaptive gradient-based block compressive sensing with sparsity for noisy images. *Multimedia Tools Appl.* **2019**, *79*, 14825–14847. [CrossRef]

28. Zhao, H.H.; Rosin, P.L.; Lai, Y.K.; Zheng, J.H.; Wang, Y.N. Adaptive block compressive sensing for noisy images. In *International Symposium on Artificial Intelligence and Robotics*; Springer: Berlin/Heidelberg, Germany, 2018; pp. 389–399.

29. Canh, T.N.; Dinh, K.Q.; Jeon, B. Edge-preserving nonlocal weighting scheme for total variation based compressive sensing recovery. In Proceedings of the 2014 IEEE International Conference on Multimedia and Expo (ICME), Chengdu, China, 14–18 July 2014; pp. 1–5. [CrossRef]

30. Li, R.; Duan, X.; Lv, Y. Adaptive compressive sensing of images using error between blocks. *Int. J. Distrib. Sens. Netw.* **2018**, *14*, 1550147718781751. [CrossRef]

31. Monika, R.; Samiappan, D.; Kumar, R. Underwater image compression using energy based adaptive block compressive sensing for IoUT applications. *Vis. Comput.* **2020**, *37*, 1499–1515. [CrossRef]

32. Gambhir, D.; Rajpal, N. Edge and Fuzzy Transform Based Image Compression Algorithm: EdgeFuzzy. In *Artificial Intelligence and Computer Vision*; Studies in Computational Intelligence; Lu, H., Li, Y., Eds.; Springer: Cham, Switzerland, 2017; Volume 672. [CrossRef]

33. Wang, J.; Wang, W.; Chen, J. Adaptive Rate Block Compressive Sensing Based on Statistical Characteristics Estimation. *IEEE Trans. Image Process.* **2021**, *31*, 734–747. [CrossRef]

34. Ferrigno, L.; Marano, S.; Paciello, V.; Pietrosanto, A. Balancing computational and transmission power consumption in Wireless Image Sensor Networks. In Proceedings of the 2005 IEEE International Conference on Virtual Environments, Human-Computer Interfaces and Measurement Systems, Messina, Italy, 18–20 July 2005; pp. 61–66.

35. Kazemi, V.; Shahzadi, A.; Bizaki, H.K. Multifocus image fusion using adaptive block compressive sensing by combining spatial frequency. *Multimedia Tools Appl.* **2022**, *81*, 15153–15170. [CrossRef]

36. Liu, Y.; Wang, L.; Cheng, J.; Li, C.; Chen, X. Multi-focus image fusion: A Survey of the state of the art. *Inf. Fusion* **2020**, *64*, 71–91. [CrossRef]

37. Mathews, J.; Nair, M.S. Adaptive block truncation coding technique using edge-based quantization approach. *Comput. Electr. Eng.* **2015**, *43*, 169–179. [CrossRef]

38. Kodak Lossless True Color Image Suite. Available online: http://www.r0k.us/graphics/Kodak (accessed on 11 October 2022).

39. CCTV Image of Leopard and Deer Images from Sanjay Gandhi National Park—Bing Images—Search. Available online: https://www.bing.com/images/feed (accessed on 1 February 2023).

40. Available online: https://github.com/ChaofWang/Awesome-Super-Resolution/blob/master/dataset.md (accessed on 10 December 2022).

41. Wang, Z.; Bovik, A.C.; Sheikh, H.R.; Simoncelli, E.P. Image Quality Assessment: From ErroVisibility to Structural Similarity. *IEEE Trans. Image Process.* **2004**, *13*, 600–612. [CrossRef]